EARTHQUAKE ENGINEERING AND STRUCTURAL DYNAMICS
Earthquake Engng Struct. Dyn. (2011)
Published online in Wiley Online Library (wileyonlinelibrary.com). DOI: 10.1002/eqe.1132

Simulation of orthogonal horizontal ground motion components for specified earthquake and site characteristics

Sanaz Rezaeian*,† and Armen Der Kiureghian‡

University of California, Berkeley, CA 94720, U.S.A.

SUMMARY

A method for generating an ensemble of orthogonal horizontal ground motion components with correlated parameters for specified earthquake and site characteristics is presented. The method employs a parameterized stochastic model that is based on a time-modulated filtered white-noise process with the filter having time-varying characteristics. Whereas the input white-noise excitation describes the stochastic nature of the ground motion, the forms of the modulating function and the filter and their parameters characterize the evolutionary intensity and nonstationary frequency content of the ground motion. The stochastic model is fitted to a database of recorded horizontal ground motion component pairs that are rotated into their principal axes, a set of orthogonal axes along which the components are statistically uncorrelated. Model parameters are identified for each ground motion component in the database. Using these data, predictive equations are developed for the model parameters in terms of earthquake and site characteristics and correlation coefficients between parameters of the two components are estimated. Given a design scenario specified in terms of earthquake and site characteristics, the results of this study allow one to generate realizations of correlated model parameters and use them along with simulated white-noise processes to generate synthetic pairs of horizontal ground motion components along the principal axes. The proposed simulation method does not require any seed recorded ground motion and is ideal for use in performance-based earthquake engineering. Copyright © 2011 John Wiley & Sons, Ltd.

Received 10 October 2010; Revised 8 March 2011; Accepted 21 March 2011

KEY WORDS: correlated components; earthquake ground motion; multi-component simulation; NGA database; performance-based earthquake engineering; principal axes; stochastic models

1. INTRODUCTION

One of the major advancements in the past decade of earthquake engineering research and practice has been the development of the concept and methodologies of performance-based earthquake engineering (PBEE) [1]. Unlike traditional building design codes that are prescriptive and only assure minimum safety and serviceability requirements, PBEE considers the entire range of seismic hazard and structural response with the overall goal of minimizing risk and life cycle costs. As a result, various levels of structural behavior, from linear to grossly nonlinear, and various levels of ground shaking, from frequent and moderate to rare and strong, must be considered in this approach. Because of these requirements, nonlinear response-history dynamic analysis, which requires knowledge of input ground motion time series, is rapidly becoming prevalent in structural engineering practice. Naturally, the validity of predicted structural responses depends on the validity of the input ground motions. Therefore, the development of ground motion time

*Correspondence to: Sanaz Rezaeian, University of California, Berkeley, CA 94720, U.S.A.
†E-mail: sanazr128@yahoo.com
‡Taisei Professor of Civil Engineering.

series that represent real ground shaking during potential future earthquakes is a crucial step in PBEE. In the current PBEE practice, input time series are selected from a database of ground motions recorded during the past earthquakes. This approach suffers from scarcity of recorded motions. Owing to this shortcoming, recorded motions are often selected from locations other than the region of interest and must be scaled in the time domain or modified in the frequency domain to match specifications of intensity or frequency content [2]. Ground motion scaling and modification methods have raised concern in the recent years, as they may easily render motions that have unrealistic characteristics [3, 4]. Using simulated ground motions to supplant or supplement recorded motions for PBEE analysis is an attractive alternative, provided the synthetic motions accurately capture those characteristics of real earthquake ground motions that are important in determining structural response.

Many ground motion simulation models have been developed in the past. Some are physics-based and employ seismological principles to model the earthquake source and propagation of seismic waves through the ground medium, e.g. [5–9]. These models typically require extensive computations and a thorough knowledge of the source, wave path, and site characteristics—information that usually is not available to the design engineer. There are also parameterized stochastic ground motion models that are fitted to recorded ground motions (e.g. [10–15] present formal reviews of older models). The majority of these models generate synthetic ground motions based on a single seed record, e.g. a ground motion recorded at the site of interest. These synthetics tend to underestimate the variability present in real earthquake ground motions. More recently, stochastic models have been developed by empirically fitting to a large number of recorded ground motions (e.g. [16–18]). However, these studies have restricted their attention to simulating single components of ground motion. In this study, we employ the stochastic model developed in [10] and the simulation method developed in [16] to formulate a new approach for simultaneous simulation of the horizontal orthogonal components of ground motion for specified earthquake and site characteristics.

The stochastic model in [10] is based on a filtered white-noise process with time-varying parameters, which relate to physical features of the ground motion, including the evolving intensity, duration, and nonstationary frequency content. The model parameters are identified by fitting statistical characteristics of the stochastic model to those of a recorded acceleration time series. In [16], this stochastic model was fitted to a large number of recorded motions and predictive equations for the model parameters in terms of earthquake and site characteristics that are readily available to a design engineer were developed. The stochastic model along with the predictive equations allow one to generate a suite of synthetic ground motions for a design earthquake that is specified in terms of the type of faulting, earthquake magnitude, source-to-site distance, and shear-wave velocity of the site of interest. Because the stochasticity of the earthquake ground motion and the variability of model parameters are properly accounted for, and because the model is calibrated to a database of recorded motions, the variability observed among the synthetics is consistent with the variability observed among real recorded ground motions. This realistic representation of ground motion variability is crucial in determining the variability of structural response, which is of interest in PBEE. A further advantage of the stochastic model used in [10, 16] and this work is that it can be directly employed for probabilistic assessment of seismic demand in PBEE by nonlinear random vibration analysis [19].

Earthquake ground motions are multi-dimensional. Despite the large number of existing ground motion simulation models, only a few are concerned with simulating multiple components. For earthquake response analysis of 3D structural systems such as bridges, dams, nuclear power plants, piping systems, or simply for 2D analysis of asymmetric structures, it is important to simulate consistent components of the ground motion. To obtain realistic synthetics, differences and similarities between the ground motion components must be carefully modeled. Considering that the ground motion components emanate from the same earthquake source and seismic waves travel through the same medium, one expects high correlations between the characteristics of the components. Some previous studies assume that the parameters of the two components are identical. For example, Yeh and Wen [20] assume the same frequency content for the component

DOI: 10.1002/eqe

of ground motion along any horizontal direction. However, they use distinct deterministic intensity envelopes for the different components, the parameters of which are identified from recorded accelerograms. Other studies that simulate ground motion components, such as Kubo and Penzien [21] or Heredia-Zavoni and Machicao-Barrionuevo [22], also use real recorded accelerograms to identify the parameters of their ground motion model, and thereby indirectly account for the correlations between parameters of the ground motion components. However, as discussed earlier, depending on a seed record is not desirable in PBEE.

In this study, we develop a method for simulating bi-directional horizontal ground motion time series for a future seismic event without the need for a seed record. Following the methods in [16], predictive equations are developed for the model parameters of each component of ground motion in terms of earthquake and site characteristics; additionally, the correlations between the parameters of the two components are empirically determined. Most existing studies that attempt to simulate ground motion components, e.g. [20–22], are based on the work of Penzien and Watabe [23] that defines an orthogonal set of principal axes, along which ground motion components are assumed to be statistically independent. In this study, we also take advantage of the concept of principal axes.

The paper begins with a brief review of the concept of principal axes of ground motions. The stochastic ground motion model in [10] is then reviewed and extended to model multiple components. Each component is modeled as a filtered white-noise process with time-varying parameters. Differences between the two component models originate from different underlying white-noise processes and from different model parameters defining their temporal and spectral characteristics. A database of ground motion components in principal directions is developed by rotating the as-recorded horizontal components of a subset of the Next Generation Attenuation (NGA) project database [24]. Based on this database, empirical predictive equations for the model parameters in terms of earthquake and site characteristics are developed and correlation coefficients between parameters of the two components are empirically determined. The outcomes allow one to randomly generate correlated model parameters for two orthogonal horizontal ground motion components along the principal axes. The generated model parameters are then used along with two statistically independent white-noise processes to simulate ground motion components. Example simulations are presented and comparisons are made of time series and response spectra of simulated and real ground motion components.

2. PRINCIPAL AXES OF GROUND MOTION

Earthquake ground motions are multi-dimensional. Neglecting the rotational components, let $a_1(t)$, $a_2(t)$, and $a_3(t)$ denote the translational components of ground acceleration along three orthogonal axes recorded at a site. Noting that the ground motion process has zero mean, the temporal correlation coefficient between a pair of components (i, j) over the time interval $\tau_1 \leqslant t \leqslant \tau_2$ is defined as

$$\rho_{a_i a_j} = \frac{\int_{\tau_1}^{\tau_2} a_i(t) a_j(t)\,\mathrm{d}t}{\sqrt{\int_{\tau_1}^{\tau_2} a_i(t)^2\,\mathrm{d}t \int_{\tau_1}^{\tau_2} a_j(t)^2\,\mathrm{d}t}} \tag{1}$$

Penzien and Watabe [23] examined this correlation coefficient for a number of recorded ground motions and observed that it did not significantly change for different time segments so that $\rho_{a_i a_j}$ could be computed for the entire length of the record (i.e. $\tau_1 = 0$ and τ_2 equals the duration of the record). The correlation coefficient naturally depends on the directions along which the motions are recorded. Penzien and Watabe [23] defined the principal axes of ground motion as the rotated axes along which the three components are uncorrelated. They further assumed that the ground motion components along these axes are statistically independent. Many subsequent studies on stochastic modeling and/or generation of synthetic ground motion components have used this definition of the principal axes, see, e.g. [20–22, 25–27]. (Although uncorrelation at the same time

DOI: 10.1002/eqe

does not necessarily imply statistical independence of two processes, this simplifying assumption has been adopted by virtually all investigators.) Furthermore, based on the examination of a small number of accelerograms, Penzien and Watabe [23] suggested that the major principal axis, i.e. the axis with the highest intensity, is horizontal and points towards the direction of the earthquake source. However, this hypothesis appears not to be supported by more recent data. In this study, we employ the above definition of the principal axes of ground motion. We do not make an assumption regarding the orientation of these axes relative to the earthquake source. Nevertheless, we assume that two principal components lie in the horizontal plane and the third in vertical. Our focus is on modeling and simulation of the two horizontal principal components. Although we do not develop the vertical component, the proposed method can be easily extended to simulate that component as well.

We distinguish the principal components in terms of their Arias intensities [28]. For an acceleration record $a(t)$, Arias intensity is a measure of the total energy and is defined by

$$I_{\mathrm{a}} = \frac{\pi}{2g} \int_0^{t_n} a^2(t)\,\mathrm{d}t \tag{2}$$

where τ_n denotes the total duration of the motion and g is the gravitational acceleration. The horizontal principal component with the larger Arias intensity is defined as the *major* principal component. Since the vertical component usually has the smallest intensity, the second horizontal principal component is denoted as the *intermediate* principal component.

As first noted by Smeby and Der Kiureghian [25], the correlation coefficient $\rho_{a_i a_j}$ between any set of rotated components depends on the difference between the intensities of the corresponding principal components. Specifically, the larger the difference between the intensities of the principal components, the higher the correlation coefficient for any given rotation angle. In the special case where the principal components have equal intensities, the correlation coefficient tends to zero for all rotation angles. An example later in Section 4 demonstrates this dependence.

3. STOCHASTIC GROUND MOTION MODEL

A good stochastic ground motion model must represent both the temporal and the spectral nonstationary characteristics of the motion. Temporal nonstationarity refers to the variation in the intensity of the motion in time, whereas spectral nonstationarity refers to the variation in its frequency content in time. Spectral nonstationarity, which is lacking in many existing stochastic ground motion models, arises from the evolving nature of seismic waves arriving at a site and is important to model, especially for nonlinear response analysis due to the moving resonant effect of inelastic and degrading structures. We refer to a stochastic model that represents both types of nonstationarities as a fully nonstationary model. It is preferred that the parameters that define the stochastic model relate to physical characteristics of the ground motion. Furthermore, the model should be parsimonious, i.e. have as few parameters as possible, and refrain from requiring extensive processing of recorded motions for parameter identification.

In this paper, we employ the stochastic ground motion model proposed in our earlier work [10], which is a fully nonstationary model and possesses the properties just mentioned. In this model, the ground acceleration process is described as the response of a linear filter with time-varying parameters to white-noise excitation. The filter response is normalized by its standard deviation and is multiplied by a deterministic time-modulating function. While modulation of the process in time introduces temporal nonstationarity, time-variation of the filter parameters provides spectral nonstationarity. Normalization by the standard deviation of the process prior to time-modulation separates the spectral and temporal nonstationary characteristics of the process, thereby greatly facilitating parameter identification. The simulated process is ultimately high-pass filtered to represent an acceleration time series. The high-pass filtering is necessary to assure zero residual velocity and displacement, as well as to produce reliable response spectral ordinates at

DOI: 10.1002/eqe

long periods. In the following, this stochastic ground motion model is extended to represent the two horizontal components of ground motion.

3.1. Model formulation

Following Rezaeian and Der Kiureghian [10], the orthogonal horizontal components of ground motion process, assumed to be Gaussian, are modeled in the continuous form by

$$x_r(t)=q(t,\boldsymbol{\alpha}_r)\left\{\frac{1}{\sigma_{hr}(t)}\int_{-\infty}^{t}h[t-\tau,\boldsymbol{\lambda}_r(\tau)]w_r(\tau)\,\mathrm{d}t\right\},\quad r=1,2 \tag{3}$$

where $x_r(t)$ is the acceleration time series of the rth component prior to high-pass filtering; $q(t,\boldsymbol{\alpha}_r)$ is a deterministic, nonnegative, time-modulating function with parameters $\boldsymbol{\alpha}_r$ controlling its shape and intensity; $w_r(\tau)$ is a white-noise process; the integral inside the curved brackets is a filtered white-noise process, where $h[t-\tau,\boldsymbol{\lambda}_r(t)]$ denotes the impulse-response function (IRF) of the filter with time-varying parameters $\boldsymbol{\lambda}_r(\tau)$; and $\sigma^2_{hr}(t)=\int_{-\infty}^{t}h^2[t-\tau,\boldsymbol{\lambda}_r(t)]\,\mathrm{d}\tau$ is the variance of the integral process, where the subscript r denotes dependence on $\boldsymbol{\lambda}_r(\tau)$. Owing to the normalization by $\sigma_{hr}(t)$, the process inside the curved brackets has unit variance and, hence, $q(t,\boldsymbol{\alpha}_r)$ equals the standard deviation of $x_r(t)$ and completely controls the temporal characteristics of the process. On the other hand, the form of the IRF and its time-varying parameters control the spectral characteristics of the process. The time-modulating function and the linear filter employed in this study are similar to those used in [16] and are summarized below.

We select a modulating function that is proportional to the gamma probability density function (PDF). Dropping the subscript r for simplicity of the notation, the function is formulated as

$$\begin{aligned} q(t,\boldsymbol{\alpha}) &= 0 \quad \text{if } t\leqslant T_0 \\ &= \alpha_1(t-T_0)^{\alpha_2-1}\exp[-\alpha_3(t-T_0)] \quad \text{if } T_0\leqslant t \end{aligned} \tag{4}$$

This modulating function has the four parameters $\boldsymbol{\alpha}=(\alpha_1,\alpha_2,\alpha_3,T_0)$, where $0<\alpha_1$ controls the intensity of the process, $1<\alpha_2$ controls its shape, $0<\alpha_3$ controls the duration of the motion, and T_0 denotes the start time of the motion. For simulation purposes, $T_0=0$ is generally selected. However, when fitting the stochastic model to a recorded ground motion, it may be necessary to set $T_0>0$. Because there is no standard as to where to set the initial point of an acceleration signal, many recorded ground motions have long stretches of zero motion in their beginning, thus requiring a value greater than zero for T_0. Proportionality of the selected modulating function to the gamma PDF allows the three parameters $(\alpha_1,\alpha_2,\alpha_3)$ to be uniquely mapped into three other parameters $(\bar{I}_\mathrm{a},D_{5-95},t_\mathrm{mid})$, which are directly related to the physical characteristics of the ground motion. $\bar{I}_\mathrm{a}$ represents the expected Arias intensity of the acceleration process:

$$\bar{I}_\mathrm{a}=E\left[\frac{\pi}{2g}\int_0^{t_n}x^2(t)\,\mathrm{d}t\right]=\frac{\pi}{2g}\int_0^{t_n}q^2(t,\boldsymbol{\alpha})\,\mathrm{d}t \tag{5}$$

D_{5-95} represents the effective duration of the motion and is defined as the time interval between the instants at which the 5 and 95% of the expected Arias intensity are reached. t_mid represents the time at the middle of the strong-shaking phase of the motion and, according to Rezaeian and Der Kiureghian [16], is defined as the time at which 45% level of the expected Arias intensity is reached. The one-to-one mapping between the parameter sets $(\alpha_1,\alpha_2,\alpha_3)$ and $(\bar{I}_\mathrm{a},D_{5-95},t_\mathrm{mid})$ is described in [16].

For the filter IRF, we select a form that corresponds to the pseudo-acceleration response of a single-degree-of-freedom linear oscillator that is given by

$$\begin{aligned} h[t-\tau,\boldsymbol{\lambda}(\tau)] &= \frac{\omega_\mathrm{f}(\tau)}{\sqrt{1-\zeta_\mathrm{f}^2(\tau)}}\exp[-\zeta_\mathrm{f}(\tau)\omega_\mathrm{f}(\tau)(t-\tau)]\sin\left[\omega_\mathrm{f}(\tau)\sqrt{1-\zeta_\mathrm{f}^2(\tau)}(t-\tau)\right] \quad \text{if } \tau\leqslant t \\ &= 0 \quad \text{otherwise} \end{aligned} \tag{6}$$

DOI: 10.1002/eqe

where $\boldsymbol{\lambda}(\tau) = (\omega_{\mathrm{f}}(\tau), \zeta_{\mathrm{f}}(\tau))$ is the set of time-varying parameters with $\omega_{\mathrm{f}}(\tau)$ denoting the frequency of the filter and $\zeta_{\mathrm{f}}(\tau)$ denoting its damping ratio. $\omega_{\mathrm{f}}(\tau)$ and $\zeta_{\mathrm{f}}(\tau)$, respectively, control the evolutionary predominant frequency and bandwidth of the process. As a simple approximation and based on the analysis of a large number of accelerograms (see [10] and [16] for details), we adopt a linear function for the filter frequency and a constant value for the filter damping ratio, i.e.

$$\omega_{\mathrm{f}}(\tau) = \omega_{\mathrm{mid}} + \omega'(\tau - t_{\mathrm{mid}}) \tag{7}$$

$$\zeta_{\mathrm{f}}(\tau) = \zeta_{\mathrm{f}} \tag{8}$$

where ω_{mid} represents the filter frequency at t_{mid}, and ω' represents the rate of change in the filter frequency with time.

Adopting the forms in (4)–(8), the horizontal ground motion components in (3) are completely defined by the set of 12 parameters $\boldsymbol{\alpha}_r = (\bar{I}_{\mathrm{a}}, D_{5-95}, t_{\mathrm{mid}})_r$ and $\boldsymbol{\lambda}_r = (\omega_{\mathrm{mid}}, \omega', \zeta_{\mathrm{f}})_r$, $r = 1, 2$. As described above, these parameters control the overall temporal and spectral characteristics of the two motions, while the white-noise processes $w_r(t)$, $r = 1, 2$, bring in the stochasticity of the motions. Naturally, one would expect that the sets of parameters for the two components be closely correlated. For horizontal components along the principal axes, the white-noise processes $w_1(t)$ and $w_2(t)$ by definition are statistically independent.

In order to facilitate digital simulation, the stochastic model in (3) is discretized in time. Let $t_i, i = 0, 1, \ldots, n$, be a set of equally spaced time points with time step Δt, where $t_0 = 0$ and t_n denotes the total duration of the motion. At a time t, $0 < t \leqslant t_n$, let $k = \mathrm{int}(t/\Delta t)$. The discretized form of (3) (identified by a hat) then is written according to Rezaeian and Der Kiureghian [10] as

$$\hat{x}_r(t) = q(t, \boldsymbol{\alpha}_r) \sum_{i=1}^{k} \{s_i(t, \boldsymbol{\lambda}_r(t_i)) u_{i,r}\}, \quad t_k \leqslant t < t_{k+1}, \quad r = 1, 2 \tag{9}$$

where $u_{i,r}$ are a set of standard normal random variables representing random pulses at the discrete time points t_i, which originate from discretization of the white-noise process $w_r(t)$. $s_i(t, \boldsymbol{\lambda}_r(t_i))$ are a set of deterministic basis functions for each component defined as

$$s_i(t, \boldsymbol{\lambda}_r(t_i)) = \frac{h[t - t_i, \boldsymbol{\lambda}_r(t_i)]}{\sqrt{\sum_{j=1}^{k} h^2[t - t_j, \boldsymbol{\lambda}_r(t_j)]}}, \quad t_k \leqslant t < t_{k+1}, \quad i = 1, \ldots, k, \quad r = 1, 2 \tag{10}$$

For a given set of model parameters, realizations of the processes in (9) are obtained by simulating the random variables $u_{i,r}$, calculating the deterministic functions $s_i(t, \boldsymbol{\lambda}_r(t_i))$ according to (10), and performing the super-positions in (9).

As mentioned earlier, the simulated stochastic process is eventually high-pass filtered. This is necessary to assure zero residual velocity and displacement of the motion, as well as to avoid the overestimation of response spectral ordinates at long periods. As in [10], a critically damped filter is selected for this purpose. Accordingly, the corrected acceleration process for the two components is obtained as the solution $\ddot{z}_r(t)$ of the differential equation

$$\ddot{z}_r(t) + 2\omega_c \dot{z}_r(t) + \omega_c^2 z_r(t) = \hat{x}_r(t), \quad r = 1, 2 \tag{11}$$

where ω_c is the frequency of the high-pass filter with a value around 0.2–$0.4\pi\,\mathrm{rad/s}$. It is noted that this filtering has little influence on the frequency content of the acceleration process beyond ω_c; therefore, in the subsequent analysis for parameter identification, characteristics of the unfiltered process $\hat{x}_r(t)$, rather than $\ddot{z}_r(t)$, are fitted to those of recorded ground motions.

3.2. Ground motion components: differences and similarities

The differences between the ground motion components, $x_1(t)$ and $x_2(t)$ as defined in (3), originate from two sources: different model parameters, i.e. $(\boldsymbol{\alpha}_1, \boldsymbol{\lambda}_1)$ and $(\boldsymbol{\alpha}_2, \boldsymbol{\lambda}_2)$, and different input excitations to the respective linear filters, i.e. the white-noise processes $w_1(\tau)$ and $w_2(\tau)$, whereas the model parameters $(\boldsymbol{\alpha}_1, \boldsymbol{\lambda}_1)$ and $(\boldsymbol{\alpha}_2, \boldsymbol{\lambda}_2)$ characterize the evolutionary intensities and frequency

DOI: 10.1002/eqe

contents of the two components, the white-noise processes $w_1(\tau)$ and $w_2(\tau)$ describe the stochastic nature of the ground motion components.

When simulating bi-directional ground motions, in addition to differences, similarities and dependencies between the two components must be accounted for. Since the ground motion components are generated from the same earthquake source and seismic waves that travel through the same medium, strong dependence between the temporal and spectral characteristics of the two components are expected. The correlation matrix $\boldsymbol{\rho}_{(\boldsymbol{\alpha}_1,\boldsymbol{\lambda}_1),(\boldsymbol{\alpha}_2,\boldsymbol{\lambda}_2)}$ between the sets of parameters, which is later estimated empirically by analyzing a large number of recorded ground motion pairs, characterizes this dependence.

As described earlier, ground motion components in general are correlated processes. Therefore, dependence between $w_1(\tau)$ and $w_2(\tau)$ must be incorporated in the model. However, if the model processes are used to describe the ground motion components along the principal axes as defined by Penzien and Watabe [23], then the two components are statistically independent and $w_1(\tau)$ and $w_2(\tau)$ can be generated as statistically independent white-noise processes.

In the following section, a database of ground motion components is developed by rotating a set of recorded ground motion pairs into their principal axes. The stochastic ground motion model is then fitted to each rotated record pair in the database and model parameters are identified. Having a database of identified model parameters, empirical predictive equations are developed for each parameter in terms of a set of earthquake and site characteristics. Furthermore, the correlation coefficients between the model parameters are empirically estimated. The predictive equations developed in this paper differ from those in [16] as they correspond to the directions of principal axes.

4. DATABASE OF PRINCIPAL GROUND MOTION COMPONENTS

The strong motion database introduced in [16] is employed. This database, which is a subset of the ground motions used in the development of Campbell–Bozorgnia NGA model [29], contains recorded motions that correspond to strike-slip or reverse types of faulting mechanism, earthquakes with moment magnitudes greater than 6.0, sites with closest distance to the ruptured area of 10–100 km, and sites with shear-wave velocity of the top 30 m of soil greater than 600 m/s. These limitations are enforced for the database to represent motions that are capable of producing nonlinear behavior in structures, and also to exclude the effects of near-fault ground motions and soil nonlinearity. Separate studies for modeling near-fault and nonlinear soil effects are underway. Each ground motion recording has two orthogonal horizontal pairs, directions of which depend on the orientation of the recording instrument. We refer to this database as the *as-recorded database* (more details and a complete list of the records are provided in [30]). The as-recorded database contains 103 pairs of horizontal recordings. In the following, each pair is rotated into directions along which the components are statistically uncorrelated, i.e. the principal axes directions. The result is a new strong motion database, which is employed in the subsequent analysis.

Let $a_1(t)$ and $a_2(t)$ represent a pair of orthogonal horizontal acceleration time series in the as-recorded directions, and $a_{1,\theta}(t)$ and $a_{2,\theta}(t)$ represent their counter-clockwise rotation by angle θ, as shown in Figure 1. This orthogonal transformation is defined by

$$\begin{bmatrix} a_{1,\theta}(t) \\ a_{2,\theta}(t) \end{bmatrix} = \begin{bmatrix} \cos(\theta) & \sin(\theta) \\ -\sin(\theta) & \cos(\theta) \end{bmatrix} \begin{bmatrix} a_1(t) \\ a_2(t) \end{bmatrix} \tag{12}$$

Every pair of as-recorded ground motion components in the database used in [16] is rotated according to (12) and the angle, $\hat{\theta}$, for which the correlation coefficient between $a_{1,\hat{\theta}}(t)$ and $a_{2,\hat{\theta}}(t)$ is zero is determined. Simple derivations show that $\hat{\theta}$ is given by

$$\hat{\theta} = \frac{1}{2}\tan^{-1}\left(\frac{2\rho_{a_1 a_2}\sigma_{a_1}\sigma_{a_2}}{\sigma_{a_1}^2 - \sigma_{a_2}^2}\right) + k\frac{\pi}{2}, \quad k = \text{integer} \tag{13}$$

DOI: 10.1002/eqe

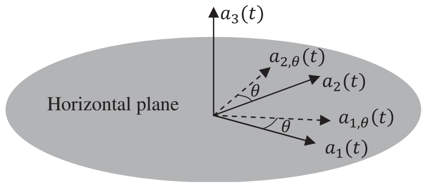

Figure 1. Rotation of orthogonal horizontal components by angle θ.

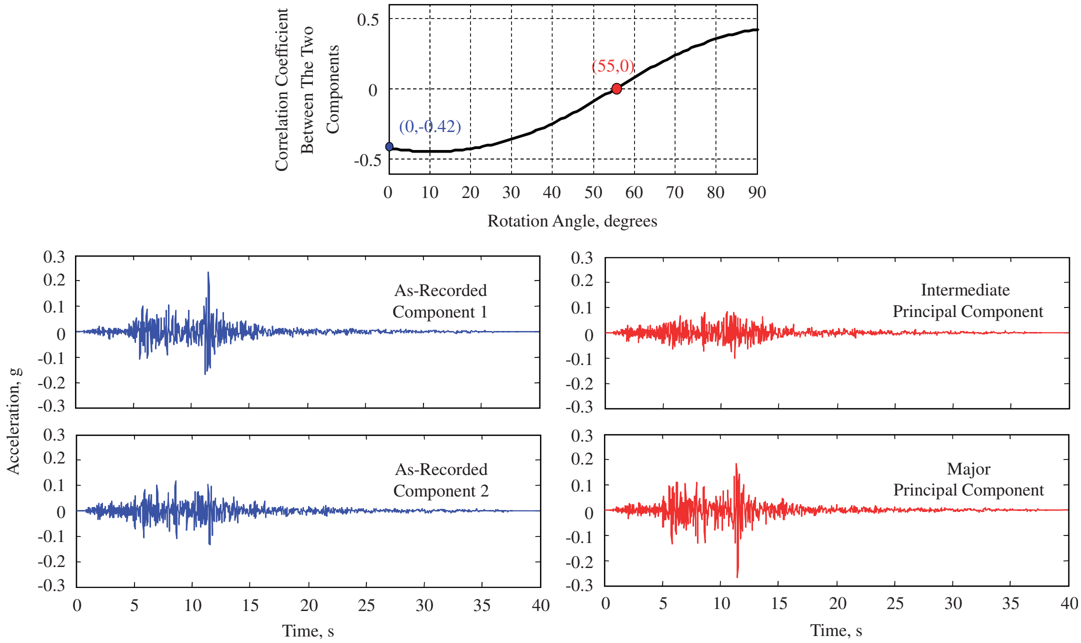

Figure 2. Horizontal as-recorded components of 1994 Northridge earthquake recorded at Mt. Wilson—CIT Station are rotated counter-clockwise. Uncorrelated principal components correspond to a rotation angle of 55°.

in which $\sigma_{a_i}^2 = \int_0^{t_n} a_i(t)^2\,\mathrm{d}t$ and k is selected such that $\hat{\theta}$ falls in the first quadrant. The corresponding rotated components, $a_{1,\hat{\theta}}(t)$ and $a_{2,\hat{\theta}}(t)$, are used to develop the database of principal ground motion components. A complete list of the correlation coefficients $\rho_{a_1a_2}$ between as-recorded components and the angles $\hat{\theta}$ for all the records in the database is presented in [30]. (The reported angles in [30] are actually for a clockwise rotation; the correct counter-clockwise angles are obtained by subtracting the reported values from 90°.)

To illustrate this analysis, two examples are presented in Figures 2 and 3. Figure 2 shows the 1994 Northridge earthquake recorded at Mt. Wilson—CIT Station. Figure 3 shows the 1999 Chi-Chi, Taiwan earthquake recorded at HW A046 Station. The components of as-recorded acceleration time series are plotted on the left side. Each pair is rotated according to (12) and the correlation coefficient between the rotated components is plotted against the rotation angle in the top chart. On the right side in each figure, the corresponding principal components of ground motion are plotted. Figures 2 and 3 clearly demonstrate the dependence of the correlation coefficient on the difference between the intensities of the principal components. The ratio between the Arias intensities of the principal components for the Northridge record in Figure 2 is 0.38, while the same measure for the Chi-Chi record in Figure 3 is 0.82. As expected, a higher ratio, which implies a smaller difference between the intensities of the principal components, results in lower overall correlations.

After obtaining the principal components, based on our earlier definition, the principal component with the larger Arias intensity is selected as the major component and the other is selected as the

DOI: 10.1002/eqe

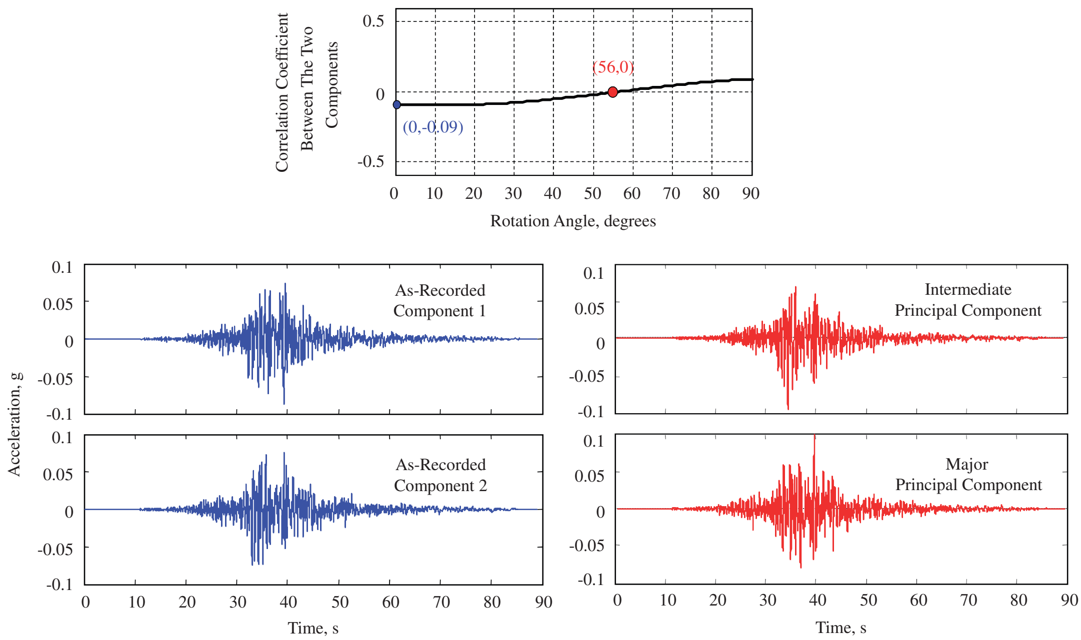

Figure 3. Horizontal as-recorded components of 1999 Chi-Chi, Taiwan earthquake at HW A046 Station are rotated counter-clockwise. Uncorrelated principal components correspond to a rotation angle of 56°.

intermediate component. This distinction is important when the correlation coefficients between model parameters of the major and intermediate components are estimated, as well as later in simulation of ground motion components.

5. IDENTIFICATION OF MODEL PARAMETERS

Sample observations of the model parameters are obtained by fitting the stochastic ground motion model in (3) to the database of principal ground motion components. This is done by fitting to the time-varying intensity and evolutionary frequency content of each component according to the methods that are described in [16] and are outlined below.

To fit the time-varying intensity of the stochastic model to that of a recorded motion, the modulating function parameters, i.e. the expected Arias intensity, $\bar{I}_a$, effective duration, D_{5-95}, and time at the middle of strong shaking, t_{mid}, are set equal to the values directly computed for the recorded accelerogram based on their definitions. The three parameters $(\alpha_1, \alpha_2, \alpha_3)$ are then calculated using the one-to-one mapping described in [16].

The filter parameters, i.e. the frequency at the middle of strong shaking, ω_{mid}, the rate of change in the frequency with time, ω', and the filter damping ratio, ζ_f, are identified by fitting to the mean zero-level up-crossing rate and the rate of change in the cumulative number of negative maxima and positive minima of the target accelerogram. Simplified procedures that were proposed in [16] are employed. Fitting to the mean zero-level up-crossing rate is performed over the time interval between 1 and 99% levels of Arias intensity, where the frequency variation is likely to be linear, resulting in the identification of parameters ω_{mid} and ω'. Fitting to the rate of change in the cumulative number of negative maxima and positive minima is performed over the time interval between 5 and 95% levels of Arias intensity, where the damping ratio is best estimated as a constant. Error measures defined in [10] are used to monitor the accuracy of identified parameters. These error measures, reported in [30], are remarkably small, verifying the adequacy of the model and the methods for identification of the filter parameters. A complete list of the

DOI: 10.1002/eqe

Table I. Summary statistical data of the identified model parameters of principal ground motion components.

Parameter	Minimum	Maximum	Sample mean	Sample standard deviation	Coefficient of variation
$I_{a,maj}$ (s g)	0.0005	2.0744	0.0646	0.2227	3.45
$I_{a,int}$ (s g)	0.0003	0.4345	0.0290	0.0648	2.24
D_{5-95} (s)	5.00	41.53	17.42	9.31	0.53
t_{mid} (s)	0.93	33.59	12.41	7.42	0.60
$\omega_{mid}/2\pi$ (Hz)	1.33	21.98	5.93	3.18	0.54
$\omega'/2\pi$ (Hz/s)	−1.437	0.382	−0.090	0.168	1.87
ζ_f	0.03	0.71	0.21	0.14	0.64

identified model parameters for all the records in the database is given in [30]. Table I presents a summary of this data.

As seen in Table I, the data for Arias intensity are divided into two groups: Arias intensity for the major principal component, $I_{a,maj}$, and Arias intensity for the intermediate principal component, $I_{a,int}$. This division reduces the number of data points for statistical analysis from 206 to 103 for each of these parameters, but this is necessary for simulation of pairs of ground motion components. Statistical analysis for the remaining model parameters is performed for the entire data set, i.e. data corresponding to the two components are combined resulting in 206 data points for each model parameter. Comparing the statistics provided in Table I to those in [16] reveals similar behavior between model parameters of principal components and model parameters of as-recorded components. The mean and standard deviation of I_a for as-recorded components were 0.0468 and 0.164 s g, respectively. As expected, $I_{a,maj}$ has a higher mean value of 0.0646 s g, and $I_{a,int}$ has a lower mean value of 0.0290 s g. Dispersion of the data for both variables $I_{a,maj}$ and $I_{a,int}$ is smaller than the dispersion of I_a for as-recorded components, i.e. the coefficients of variation of $I_{a,maj}$ and $I_{a,int}$ are 3.45 and 2.24, respectively, versus a coefficient of variation of 3.50 for I_a of as-recorded components. This smaller dispersion is expected because of the sorting of the intensities of the principal components.

Probability distribution models are assigned to each of the six stochastic model parameters. The forms of these distributions are inferred by visually inspecting the histograms of the identified model parameters and examining the fit of the corresponding empirical cumulative distribution functions. Parameters of the chosen distributions are then estimated by the method of maximum likelihood. In the event that several alternatives exist for the distribution of a model parameter, standard statistical goodness-of-fit tests are performed to identify the best alternative. Distribution types and their assigned boundaries are presented in Table II. For $\omega'/2\pi$, the fitted distribution is a two-sided truncated exponential with the PDF

$$f_{\omega'/2\pi}(\omega'/2\pi)=\begin{cases}5.38\exp(7.26\omega'/2\pi), & -2<\omega'/2\pi<0\\ 5.38\exp(-20.77\omega'/2\pi), & 0<\omega'/2\pi<0.5\\ 0 & \text{otherwise}\end{cases} \tag{14}$$

Compared to the as-recorded database (see [16]), the lower boundary of the beta distribution assigned to D_{5-95} has dropped from 5 to 4 s, and the upper boundary of the beta distribution assigned to t_{mid} has decreased from 40 to 35 s. These are insignificant differences.

Figures 4 and 5 show the assigned marginal PDFs superimposed on the normalized frequency diagrams of the model parameters. In these figures, the fitted PDFs corresponding to the as-recorded database (from [16]) are also plotted (dashed lines) for comparison. Again, differences are insignificant.

6. EMPIRICAL PREDICTIVE EQUATIONS FOR THE MODEL PARAMETERS

For PBEE analysis, it is desirable to have a stochastic ground motion model parameterized in terms of information that is available to an engineer for a given earthquake design scenario.

DOI: 10.1002/eqe

Table II. Distribution models assigned to stochastic model parameters.

Parameter	Fitted distribution (means and standard deviations are according to columns 4 and 5 of Table I)	Distribution bounds
$\bar{I}_{a,\mathrm{major}}$ (s g)	Lognormal	$(0,\infty)$
$\bar{I}_{a,\mathrm{inter}}$ (s g)	Lognormal	$(0,\infty)$
D_{5-95} (s)	Beta	$[4,45]$
t_{mid} (s)	Beta	$[0.5,35]$
$\omega_{\mathrm{mid}}/2\pi$ (Hz)	Gamma	$(0,\infty)$
$\omega'/2\pi$ (Hz/s)	Two-sided truncated exponential (14)	$[-2,0.5]$
ζ_{f}	Beta	$[0.02,1]$

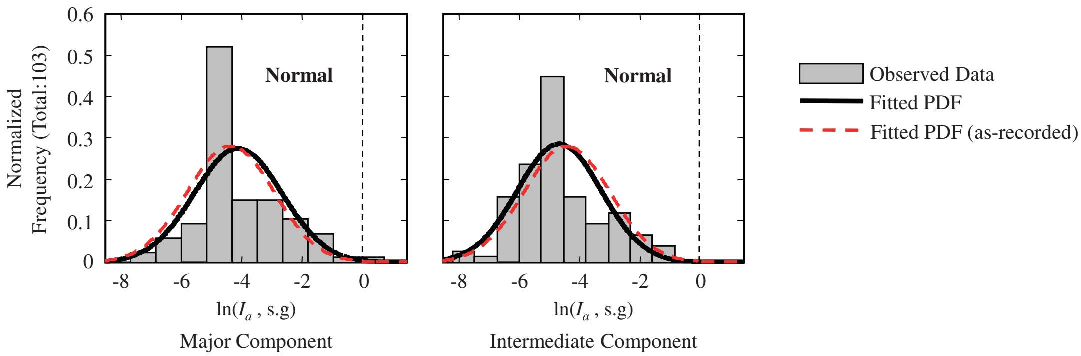

Figure 4. Normalized frequency diagrams of the identified Arias intensities for the major and intermediate components of records in the principal ground motion components database. Fitted probability density functions are superimposed.

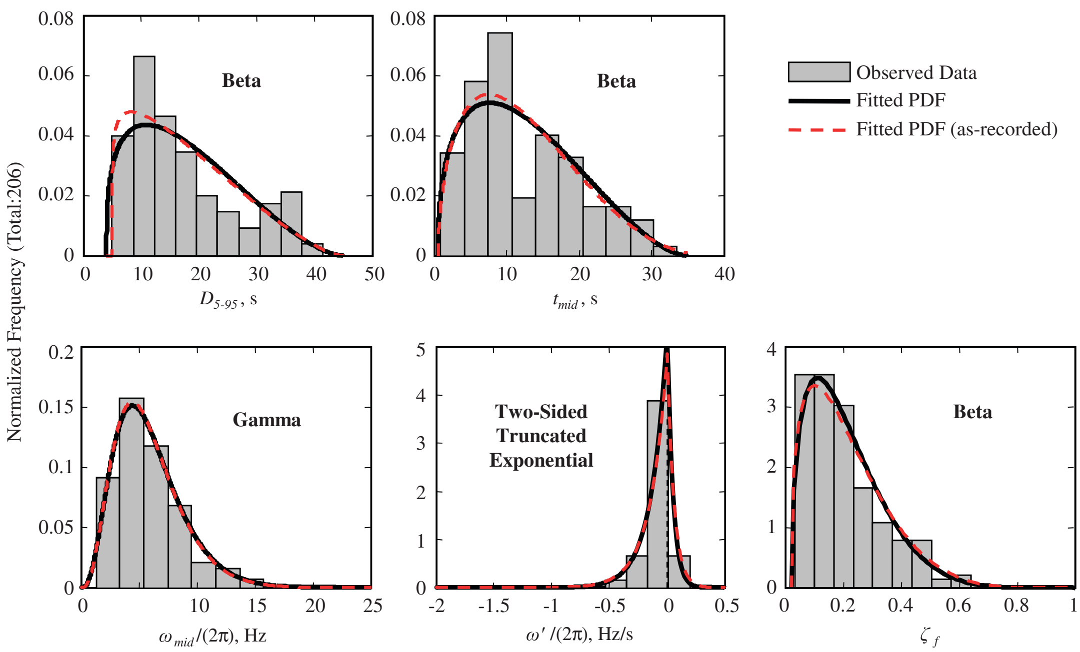

Figure 5. Normalized frequency diagrams of the identified model parameters for the principal ground motion components database. Data corresponding to major and intermediate components are combined. Fitted probability density functions are superimposed.

DOI: 10.1002/eqe

Four variables that describe the earthquake and site characteristics and are commonly used to describe a design scenario are selected. These variables are denoted by F, M, R_{rup}, and V_{S30} and respectively represent the faulting mechanism, the moment magnitude, the closest distance from the site to the ruptured area, and the shear-wave velocity at the top 30 m of the site. Following the constraints of the selected ground motion database, F assumes the values of 0 and 1 for strike-slip and reverse types of faulting, $6.0 \leqslant M$, $10\,\mathrm{km} \leqslant R_{\mathrm{rup}} \leqslant 100\,\mathrm{km}$, and $600\,\mathrm{m/s} \leqslant V_{S30}$. In this section, random-effects regression modeling is performed on the database of identified stochastic model parameters to relate them to the four earthquake variables. As a result, predictive equations of the form

$$\Phi^{-1}[F_p(p)] = \mu(F, M, R_{\mathrm{rup}}, V_{S30}, \boldsymbol{\beta}) + \eta + \in \tag{15}$$

are developed that express a model parameter, p (i.e. one of the parameters listed in Table II), in terms of $(F, M, R_{\mathrm{rup}}, V_{S30})$. On the left-hand side of (15), $\Phi^{-1}[\cdot]$ is the inverse of the standard normal cumulative distribution function and $F_p(\cdot)$ is the cumulative distribution function of p as reported in Table II. $\upsilon = \Phi^{-1}[F_p(p)]$, which represents the transformation of a model parameter into the standard normal space, satisfies the normality criterion required for the response variable in regression analysis. On the right-hand side of (15), $\mu(\cdot)$ represents the predicted mean of υ conditioned on earthquake and site characteristics and involving the set of regression coefficients $\boldsymbol{\beta}$, and $\eta + \in$ represents the total regression error defined as the difference between the observed and predicted values. Because the database contains different numbers of recordings for different earthquakes, random-effects regression is employed so that the results are not overly influenced by an individual earthquake with many records. This requires the regression error to be divided into two components η and $\in$, which are both independent zero-mean normally distributed random variables having variances τ^2 and σ^2, respectively. η represents the error among data belonging to different earthquakes, the inter-event error, and $\in$ represents the error among the data belonging to records of an individual earthquake, the intra-event error. Each earthquake is expected to have its own particular effect on its resulting ground motions. This effect, which is random and varies from earthquake to earthquake, is captured by the inter-event error. The selected method of regression effectively handles the problem of weighing observations and, unlike ordinary regression analysis, properly accounts for the statistical dependence of multiple observations from individual earthquakes.

Once regression models (15) are developed for the model parameters, they are used to generate random realizations of these parameters. These are then used together with random realizations of white-noise processes in the stochastic model in (9) to generate random realizations of the ground motion components. This process is described in detail in Section 7.

6.1. Regression results

Considering the relatively narrow range of earthquake magnitudes, a linear form of the regression equation for each transformed model parameter in terms of explanatory functions representing the type of faulting, earthquake magnitude, source-to-site distance, and soil effects is employed. Furthermore, homoscedasticity is assumed, i.e. the variances of the error terms η and $\in$ are assumed to be independent of the variables F, M, R_{rup}, and V_{S30}. Various linear and nonlinear forms of the explanatory functions were examined. To estimate the regression coefficients and variance components, the maximum-likelihood technique described in [16] was employed. For each model parameter, the relative performances of the resulting functional forms were assessed by inspecting the residuals and the estimates of the variance components. The functional forms with smaller variances that demonstrated adequate behavior of the residuals, i.e. lack of systematic patterns in the plots of residuals versus the predictor variables, were selected. The resulting predictive equations are given in (16) and (17). In these equations, $i = 1_{\mathrm{maj}}, 1_{\mathrm{int}}, 2, \ldots, 6$ indexes the transformed model parameters υ_i. This set of indexes corresponds to $\bar{I}_{\mathrm{a,maj}}, \bar{I}_{\mathrm{a,int}}, D_{5-95}, t_{\mathrm{mid}}, \omega_{\mathrm{mid}}/2\pi, \omega'/2\pi$, and ζ_{f},

DOI: 10.1002/eqe

Table III. Maximum-likelihood estimates of regression coefficients and standard error components.

i	$\beta_{i,0}$	$\beta_{i,1}$	$\beta_{i,2}$	$\beta_{i,3}$	$\beta_{i,4}$	τ_i	σ_i	P-Value
1_{maj}	−1.841	0.008	**3.065**	**−1.351**	−0.168	0.176	0.614	0.000
1_{int}	−2.408	−0.073	**3.307**	**−1.295**	−0.246	0.474	0.583	0.000
2	−5.859	**−0.707**	**6.472**	**0.231**	**−0.565**	0.475	0.577	0.000
3	−5.038	**−0.296**	**4.614**	**0.350**	−0.175	0.495	0.431	0.000
4	2.086	−0.041	−1.660	**−0.217**	0.037	0.696	0.714	0.001
5	−3.224	0.067	**3.262**	0.029	−0.144	0.168	0.921	0.019
6	0.692	**−0.676**	0.296	**−0.341**	0.181	0.704	0.709	0.000

respectively

$$v_i=\beta_{i,0}+\beta_{i,1}(F)+\beta_{i,2}\left(\frac{M}{7.0}\right)+\beta_{i,3}\left(\ln\frac{R_{\text{rup}}}{25\,\text{km}}\right)+\beta_{i,4}\left(\ln\frac{V_{S30}}{750\,\text{m/s}}\right)+\eta_i+\epsilon_i,\quad i=1_{\text{maj}},1_{\text{int}} \tag{16}$$

$$v_i=\beta_{i,0}+\beta_{i,1}(F)+\beta_{i,2}\left(\frac{M}{7.0}\right)+\beta_{i,3}\left(\frac{R_{\text{rup}}}{25\,\text{km}}\right)+\beta_{i,4}\left(\frac{V_{S30}}{750\,\text{m/s}}\right)+\eta_i+\epsilon_i,\quad i=2,\dots,6 \tag{17}$$

The maximum-likelihood estimates of the regression coefficients and variance components are presented in Table III. For each predictive equation, standard significance test on the linear regression formula is performed, i.e. F-test with the null hypothesis $\beta_{i,1}=\beta_{i,2}=\beta_{i,3}=\beta_{i,4}=0$. The P-values are reported in Table III. The regression coefficients $\beta_{i,1}, \beta_{i,2}, \beta_{i,3}$, and $\beta_{i,4}$ were individually tested ($\beta_{i,0}$ was skipped because inclusion of a constant term in the regression formulation was not questioned), i.e. t-test with the null hypothesis $\beta_{i,j}=0,\ j=1,\dots,4$. Those coefficients with statistical significance at the 95% confidence level are shown in bold in Table III. However, regardless of the significance level, all the coefficients are used later in the simulation.

Comparisons of estimated regression coefficients and variance components to those in [16], which employed the as-recorded database and only modeled one component of ground motion, for the most part reveal insignificant differences. One important difference, however, originates from developing separate predictive equations for $\bar{I}_{\text{a,maj}}$ and $\bar{I}_{\text{a,int}}$ in this study, as opposed to the one equation for $\bar{I}_{\text{a}}$ in [16], which was sufficient for modeling one component of ground motion.

6.2. *Correlation analysis*

An important result of this study is the correlation matrix between the model parameters of the major and intermediate principal components. This correlation matrix is presented in Table IV. The correlation coefficient between two (transformed) model parameters is estimated empirically as the sample correlation coefficient between their corresponding total residuals. Again homoscedasticity is assumed, i.e. the correlation coefficient is assumed to be independent of F, M, R_{rup}, and V_{S30}. Observe that the off-diagonal block in Table IV, which represents the correlation coefficients between the transformed model parameters of the major and intermediate components, contains high numbers. Namely, the correlation coefficients between pairs of similar model parameters of the two components are 0.92 for v_1 (corresponding to the Arias intensities), 0.89 for v_2 (corresponding to the effective durations), 0.96 for v_3 (corresponding to t_{mid} values), 0.94 for v_4 (corresponding to ω_{mid} values), 0.52 for v_5 (corresponding to ω' values), and 0.75 for v_6 (corresponding to ζ_{f} values). High correlations are also observed between different model parameters of the two components. For example, a correlation of 0.68 is observed between v_3 of the intermediate component (corresponding to t_{mid}) and v_2 of the major component (corresponding to the effective duration). These high correlations should not be neglected in simulation of ground motion components.

The diagonal blocks in Table IV represent correlation coefficients between model parameters of the individual components. Observe that the two diagonal blocks are not significantly different

DOI: 10.1002/eqe

Table IV. Estimated correlation coefficients between transformed model parameters of two horizontal principal ground motion components.

		Major component						Intermediate component					
		v_1	v_2	v_3	v_4	v_5	v_6	v_1	v_2	v_3	v_4	v_5	v_6
Major component	v_1	1											
	v_2	−0.38	1										
	v_3	−0.04	+0.68	1									
	v_4	−0.21	−0.07	−0.24	1					Sym.			
	v_5	−0.25	−0.21	−0.22	1								
	v_6	−0.06	−0.26	−0.26	+0.28	−0.06	1						
Intermediate component	v_1	+0.92	−0.31	+0.04	−0.13	+0.19	−0.01	1					
	v_2	−0.30	+0.89	+0.65	−0.15	−0.21	−0.23	−0.31	1				
	v_3	−0.03	+0.68	+0.96	−0.29	−0.22	−0.29	+0.01	+0.69	1			
	v_4	−0.13	−0.17	−0.30	+0.94	−0.10	+0.32	−0.08	−0.20	−0.34	1		
	v_5	+0.09	−0.11	−0.24	−0.10	+0.52	−0.02	+0.07	−0.18	−0.24	−0.19	1	
	v_6	+0.02	−0.17	−0.21	+0.29	−0.13	+0.75	−0.00	−0.17	−0.22	+0.29	−0.05	1

from each other; they are also not significantly different from correlation coefficients estimated for a single component in [16] based on the as-recorded database.

7. SIMULATION OF PRINCIPAL COMPONENTS OF GROUND MOTION

Given a design scenario that is defined by the set of earthquake and site characteristics F, M, R_{rup}, and V_{S30}, any number of synthetic ground motion pairs can be generated in the directions of principal axes by randomly simulating sets of 12 model parameters (six for each component), using them in (9) along with two statistically independent white-noise processes, and post-processing according to (11). This procedure does not require any previously recorded seed motions and is ideal for use in PBEE. Furthermore, it preserves the natural variability of real ground motions for the given design scenario because not only the stochasticity of ground motion time series, but also the variability of model parameters are properly accounted for.

To randomly simulate one set of model parameters, we assume that the 12 transformed model parameters, $(v_i)_r,\ i=1,\ldots,6,\ r=1,2$, for the major and intermediate components, are jointly normal random variables with means $\mu_i(F, M, R_{\text{rup}}, V_{S30}, \boldsymbol{\beta}_i)$, variances $\tau_i^2+\sigma_i^2$, and correlation coefficients as given in Table IV. This is equivalent to assuming that the 12 model parameters in the physical space $(\bar{I}_{\text{a}}, D_{5-95}, t_{\text{mid}}, \omega_{\text{mid}}, \omega', \zeta_{\text{f}})_r,\ r=1,2$, for the major and intermediate components have the Nataf joint distribution [31] with the marginal distributions specified in Table II. Due to the dependence of the means on F, M, R_{rup}, and V_{S30}, the joint distribution is conditioned on the earthquake and site characteristics. Given a set of earthquake and site characteristics, transformed model parameters are first simulated as jointly normal random variables with above means, variances, and correlation coefficients. The set of realizations $(v_1,\ldots,v_6)_r,\ r=1,2$, are then transformed back to their physical spaces using the inverse transform $p=F_p^{-1}[\Phi(v)]$, where p represents a model parameter in the physical space and v represents the corresponding simulated value in the standard normal space. The result is a set of realizations of the model parameters $(\bar{I}_{\text{a}}, D_{5-95}, t_{\text{mid}}, \omega_{\text{mid}}, \omega', \zeta_{\text{f}})_r,\ r=1,2$. The first three parameters of each component are converted into the modulating function parameters, yielding the set of realizations $(\alpha_1, \alpha_2, \alpha_3, \omega_{\text{mid}}, \omega', \zeta_{\text{f}})_r$, $r=1,2$. These parameter values together with two sets, one for each component, of n statistically independent standard normal random variables $u_{i,r}, i=1,\ldots,n,\ r=1,2$, are used in (9) to generate a pair of synthetic accelerograms $\hat{x}_{\text{maj}}(t)$ and $\hat{x}_{\text{int}}(t)$. These are then used in (11) to generate the corrected accelerograms $\ddot{z}_{\text{maj}}(t)$ and $\ddot{z}_{\text{int}}(t)$. Any number of synthetic accelerogram pairs for the given earthquake and site characteristics can be generated by simulating new realizations of $(v_i)_r,\ i=1,\ldots,6$ and $u_{i,r},\ i=1,\ldots,n,\ r=1,2$.

DOI: 10.1002/eqe

Since by definition the Arias intensity of the major component must be greater than the Arias intensity of the intermediate component, simulation of the parameters must satisfy this condition. Because predictive equations were developed for sorted Arias intensities of the two principal components, the probability that randomly generated parameters will satisfy the condition $\bar{I}_{\mathrm{a,maj}} > \bar{I}_{\mathrm{a,int}}$ is high. A simple way to observe the required relationship is to simply discard the small subset of simulations with $\bar{I}_{\mathrm{a,maj}} < \bar{I}_{\mathrm{a,int}}$. In our case, this amounted to 1–2% of the simulations. This essentially conditions the joint probability distribution of the model parameters on the event $\bar{I}_{\mathrm{a,maj}} > \bar{I}_{\mathrm{a,int}}$.

As an example application, Figure 6 shows pairs of acceleration, velocity, and displacement time series of the major and intermediate components for one recorded and two simulated ground motions. The simulated motions are generated for the earthquake and site characteristics of the recorded motion. Observe that, for each pair, simulated components are different but have similar overall characteristics in the same manner as the recorded pair of motions, i.e. the two components have entirely different time series but have similar intensity evolution, duration, predominant frequency, and bandwidth. These similarities are also apparent in the model parameters, which are listed in Table V for each component of the recorded and simulated ground motions. In general, similar model parameters for simulated principal components are closer in value to each other than to the parameters of another simulated pair.

7.1. Comparison of elastic response spectra with real ground motions

In this section we compare the elastic response spectra of synthetic ground motion pairs with those of a recorded pair. In addition to verifying the validity of the synthetic response spectral shapes, this comparison allows the assessment of the variability among synthetic ground motions simulated for a specified set of earthquake and site characteristics. To demonstrate this, 50 synthetic principal ground motion pairs are generated for the earthquake and site characteristics of the recorded motion pair in Figure 3. The 5% damped elastic response spectra of the synthetics are then compared to those of the recorded pair in Figure 7. At a given spectral period, we expect the spectral ordinates of the pair of recorded motions to fall within the range predicted by the synthetics. This result is expected because the recorded ground motion pair is only one realization of all the possible ground motions for the specified earthquake and site characteristics, and because the suite of generated synthetic motions properly accounts for the natural variability of real earthquake ground motions. As can be seen in Figure 7, the response spectra of the recorded components fall well within the spread of synthetic response spectra. Furthermore, by comparison with the recorded spectra, the synthetics appear to have reasonable shapes, including at the long-period range.

In [16], the statistics of the elastic response spectra of sets of single-component synthetic ground motions for various magnitude and source-to-site distances were compared to their corresponding predicted values by four of the NGA models [24] that are commonly used in engineering practice. It was concluded that the median and variability of elastic response spectra (at given spectral periods) for synthetics were in close agreement with those of the NGA models. As previously mentioned, the predictive equations in (16) and (17) are similar to those developed in [16] for a single component of ground motion. Furthermore, the regression coefficients and the fitted marginal distributions presented in Tables II and III are not significantly different from those in [16]. These are the factors that determine the median and variability of synthetic response spectra. Therefore, we may conclude that the ground motion simulation method presented in this paper is still compatible with the NGA models, but has the important advantage of simultaneously simulating two horizontal components instead of a randomly oriented component.

8. USE OF SIMULATED PRINCIPAL COMPONENTS IN DESIGN

The method presented in the preceding sections allows the generation of synthetic horizontal ground motion components in the principal directions. In using these components for safety assessment or design of structures, decision must be made as to the orientation of the simulated principal

DOI: 10.1002/eqe

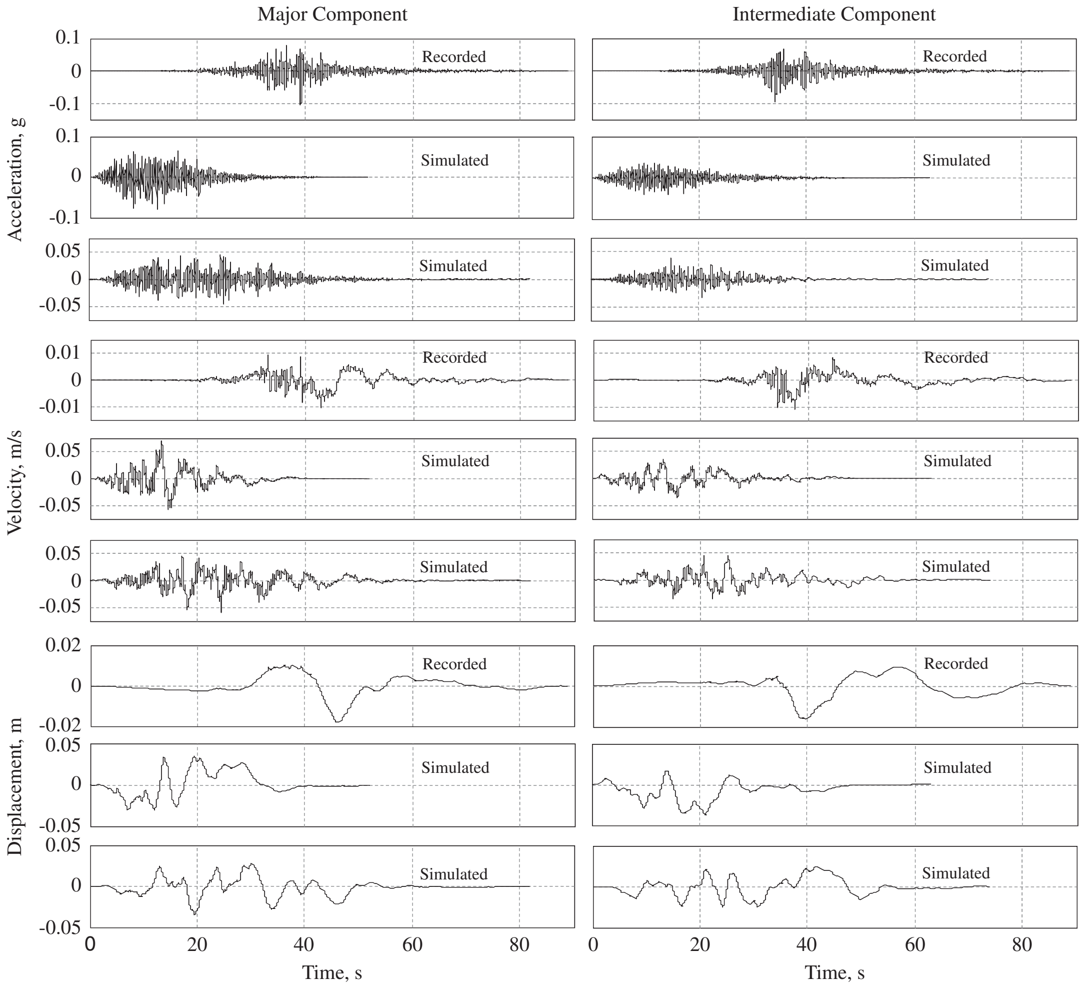

Figure 6. Pairs of acceleration, velocity, and displacement time series of one recorded (same as in Figure 3) and two simulated ground motion components along principal directions. Model parameters for each record are listed in Table V. All motions correspond to $F=1$, $M=7.62$. $R_{\text{rup}}=51.8\,\text{km}$ and $V_{S30}=618\,\text{m/s}$.

Table V. Realizations of the model parameters for ground motion components in Figure 6.

	Realizations of model parameters											
	Major component						Intermediate component					
	I_a (s g)	D_{5-95} (s)	t_{mid} (s)	$\omega_{\text{mid}}/2\pi$ (Hz)	$\omega'/2\pi$ (Hz/s)	ζ_f	I_a (s g)	D_{5-95} (s)	t_{mid} (s)	$\omega_{\text{mid}}/2\pi$ (Hz)	$\omega'/2\pi$ (Hz/s)	ζ_f
Recorded	0.0165	16.7	18.3	3.9	−0.08	0.12	0.0135	17.0	17.8	4.1	−0.02	0.11
Simulated	0.0147	17.3	10.1	8.1	−0.12	0.42	0.0047	21.0	10.7	8.6	−0.18	0.50
Simulated	0.0099	27.2	17.1	3.2	−0.03	0.20	0.0034	24.8	16.9	3.7	−0.13	0.35

components relative to the input directions of the structure. We see at least four alternatives: (a) Orient the principal components such that the major principal component aligns with the weak direction of the structure. This would tend to give conservative results for most response quantities. (b) Consider all possible orientations and select the one that is most critical for each response quantity of interest. If the analysis is linear, the critical direction for each response quantity can

DOI: 10.1002/eqe

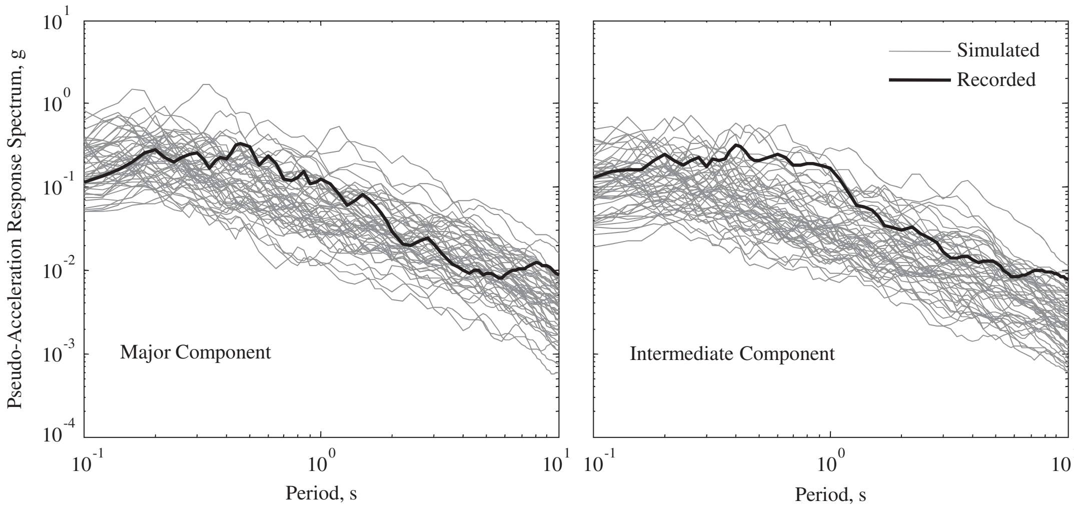

Figure 7. Elastic response spectra (5% damped) of principal components of the recorded motion in Figure 3 and of 50 synthetic motions generated for the earthquake and site characteristics of the recorded motion.

be obtained in closed form (see [25–27]). However, for nonlinear analysis, this angle must be determined by numerical investigation. This approach clearly will give the most conservative design. (c) Consistent with the philosophy of a probabilistic approach, if the orientation of the principal components is unknown, the angle relative to the input directions of the structure can be randomly selected. This selection would be appropriate in a simulation approach aimed at probabilistic characterization of the response. (d) If the Penzien and Watabe [23] hypothesis regarding the major principal component being directed towards the earthquake source is adopted, then that determines the orientation of the principal axes, provided the location of the potential earthquake source is known. In each of the cases (b)–(d), if desired, the simulated principal components can be rotated onto the input directions of the structure by use of the orthogonal transformation in (12) for convenience of the analysis.

9. CONCLUSION

A method is presented for simulating an ensemble of synthetic orthogonal horizontal ground motion components for specified earthquake and site characteristics. A new ground motion database is constructed by rotating recorded horizontal ground motion component pairs into their principal axes, i.e. the orthogonal axes along which the components are statistically uncorrelated. A previously developed stochastic ground motion model is extended to describe two principal components and the model parameters are identified by fitting to each recorded pair in the new database. Using the database of identified model parameters and random-effects regression analysis, predictive equations are developed that express each model parameter in terms of variables defining a set of earthquake and site characteristics, which are typically available to the design engineer. Correlation coefficients between the model parameters of the two components are empirically estimated by analysis of the regression residuals. As expected, the correlation coefficients between similar parameters of the two components are high, as they characterize the similarity between overall characteristics of the two components.

The proposed modeling and simulation procedure can be applied to any database of recorded ground motions. Considering the database utilized in this study, the predictive equations developed in this study are only applicable for shallow crustal earthquakes in tectonically active regions with $6.0 \leqslant M$, $10\,\text{km} \leqslant R_{\text{rup}} \leqslant 100\,\text{km}$, and $600\,\text{m/s} \leqslant V_{S30}$. The stochastic model, the predictive equations, and the estimated correlation coefficients are utilized to simulate horizontal ground motion

DOI: 10.1002/eqe

components along the principal axes. Examples are presented that compare the acceleration, velocity, and displacement time series, as well as elastic response spectra of synthetic and recorded ground motion pairs. The synthetic components can be rotated into any desired direction, e.g. the input axes of a structure. Importantly, the synthetic ground motions preserve the natural variability present in real ground motions for a given set of earthquake and site characteristics. As such, they can be used to estimate the statistics of structural response in the context of performance-based earthquake engineering, particularly when the analysis requires specification of multi-component ground motions. Although not done here, the method presented in this paper can be easily extended to also simulate the vertical component of ground motion.

ACKNOWLEDGEMENTS

This work was supported by the State of California through the Transportation Systems Research Program of the Pacific Earthquake Engineering Research Center (PEER). Any opinions, findings, and conclusions or recommendations expressed in this material are those of the authors and do not necessarily reflect those of the funding agency. Special thanks are due Dr Yousef Bozorgnia, the executive director of PEER, for his support and valuable advice during the course of this study.

REFERENCES

1. Bozorgnia Y, Bertero VV (eds). *Earthquake Engineering*: *From Engineering Seismology to Performance-based Engineering*. CRC Press: Boca Raton, FL, 2004.
2. Goulet CA, Watson-Lamprey J, Baker JW, Haselton CB, Luco N. Assessment of ground motion selection and modification (GMSM) methods for non-linear dynamic analyses of structures. *Geotechnical Earthquake Engineering and Soil Dynamics IV* (*GSP 181*), Sacramento, CA, 2008.
3. Luco N, Bazzurro P. Does amplitude scaling of ground motion records result in biased nonlinear structural drift responses? *Earthquake Engineering and Structural Dynamics* 2007; **36**:1813–1835.
4. Naeim F, Lew M. On the use of design spectrum compatible time histories. *Earthquake Spectra* 1995; **11**:111–127.
5. Ameri G, Gallovic F, Pacor F, Emolo A. Uncertainties in strong ground-motion prediction with finite-fault synthetic seismograms: an application to the 1984 M 5.7 Gubbio, Central Italy, earthquake. *Bulletin of the Seismological Society of America* 2009; **99**:647–663.
6. Frankel A. A constant stress-drop model for producing broadband synthetic seismograms: comparison with the next generation attenuation relations. *Bulletin of the Seismological Society of America* 2009; **99**:664–680.
7. Causse M, Cotton F, Cornou C, Bard PY. Calibrating median and uncertainty estimates for a practical use of empirical Green's functions technique. *Bulletin of the Seismological Society of America* 2008; **98**:344–353.
8. Liu P, Archuleta RJ, Hartzell SH. Prediction of broadband ground-motion time histories: hybrid low/high-frequency method with correlated random source parameters. *Bulletin of the Seismological Society of America* 2006; **96**:2118–2130.
9. Boore DM. Simulation of ground motion using the stochastic method. *Pure and Applied Geophysics* 2003; **160**:635–676.
10. Rezaeian S, Der Kiureghian A. A stochastic ground motion model with separable temporal and spectral nonstationarities. *Earthquake Engineering and Structural Dynamics* 2008; **37**:1565–1584.
11. Conte JP, Peng BF. Fully nonstationary analytical earthquake ground-motion model. *Journal of Engineering Mechanics* (ASCE) 1997; **12**:15–24.
12. Kozin F. Autoregressive moving average models of earthquake records. *Probabilistic Engineering Mechanics* 1988; **3**:58–63.
13. Shinozuka M, Deodatis G. Stochastic process models for earthquake ground motion. *Probabilistic Engineering Mechanics* 1988; **3**:114–123.
14. Ahmadi G. Generation of artificial time-histories compatible with given response spectra—a review. *Solid Mechanics Archives* 1979; **4**:207–239.
15. Liu SC. Synthesis of stochastic representations of ground motions. *Bell Systems Technical Journal* 1970; **49**: 521–541.
16. Rezaeian S, Der Kiureghian A. Simulation of synthetic ground motions for specified earthquake and site characteristics. *Earthquake Engineering and Structural Dynamics* 2010; **39**:1155–1180.
17. Pousse G, Bonilla LF, Cotton F, Margerin L. Nonstationary stochastic simulation of strong ground motion time histories including natural variability: application to the K-net Japanese database. *Bulletin of the Seismological Society of America* 2006; **96**:2103–2117.
18. Alamilla L, Esteva L, Garcia-Perez J, Diaz-Lopez O. Evolutionary properties of stochastic models of earthquake accelerograms: their dependence on magnitude and distance. *Journal of Seismology* 2001; **5**:1–21.
19. Fujimura K, Der Kiureghian A. Tail-equivalent linearization method for nonlinear random vibration. *Probabilistic Engineering Mechanics* 2007; **22**:63–76.

DOI: 10.1002/eqe

20. Yeh CH, Wen YK. Modeling of nonstationary earthquake ground motion and biaxial and torsional response of inelastic structures. Civil Engineering Studies. *Structural Research Series Report No. 546*, University of Illinois, 1989.
21. Kubo T, Penzien J. Simulation of three-dimensional strong ground motions along principal axes, San Fernando earthquake. *Earthquake Engineering and Structural Dynamics* 1979; **7**:279–294.
22. Heredia-Zavoni E, Machicao-Barrionuevo R. Response to orthogonal components of ground motion and assessment of percentage combination rules. *Earthquake Engineering and Structural Dynamics* 2004; **33**:271–284.
23. Penzien J, Watabe M. Characteristics of 3-dimensional earthquake ground motions. *Earthquake Engineering and Structural Dynamics* 1975; **3**:365–373.
24. Abrahamson NA, Atkinson G, Boore D, Bozorgnia Y, Campbell K, Chiou B, Idriss IM, Silva W, Youngs R. Comparisons of the NGA ground-motion relations. *Earthquake Spectra* 2008; **24**:45–66.
25. Smeby W, Der Kiureghian A. Modal combination rules for multicomponent earthquake excitation. *Earthquake Engineering and Structural Dynamics* 1985; **13**:1–12.
26. Lopez OA, Chopra AK, Hernandez JJ. Critical response of structures to multicomponent earthquake excitation. *Earthquake Engineering and Structural Dynamics* 2000; **29**:1759–1778.
27. Menun C, Der Kiureghian A. A replacement for the 30%, 40% and SRSS rules for multi-component seismic analysis. *Earthquake Spectra* 1998; **14**:153–163.
28. Arias A. A measure of earthquake intensity. In *Seismic Design for Nuclear Power Plants*, Hansen RJ (ed.). MIT Press: Cambridge, MA, 1970; 438–483.
29. Campbell KW, Bozorgnia Y. NGA ground motion model for the geometric mean horizontal component of PGA, PGV, PGD and 5% damped linear elastic response spectra for periods ranging from 0.01 to 10 s. *Earthquake Spectra* 2008; **24**:139–171.
30. Rezaeian S, Der Kirureghian A. Stochastic modeling and simulation of ground motions for performance-based earthquake engineering. *PEER Report 2010/02*, Pacific Earthquake Engineering Research Center, 2010.
31. Liu PL, Der Kiureghian A. Multivariate distribution models with prescribed marginals and covariances. *Probabilistic Engineering Mechanics* 1986; **1**:105–112.

DOI: 10.1002/eqe